

2026

Effect of zirconia nanopowders as functional fillers in dental adhesives on bonding durability and wear resistance to zirconia substrates

Ting-Hsun Lan

Chin-Yun Pan

Yu-Feng Chen

Chia-I Tiffany Yin

Follow this and additional works at: <https://jds.ads.org.tw/journal>

Recommended Citation

Lan, Ting-Hsun; Pan, Chin-Yun; Chen, Yu-Feng; and Yin, Chia-I Tiffany (2026) "Effect of zirconia nanopowders as functional fillers in dental adhesives on bonding durability and wear resistance to zirconia substrates," *Journal of Dental Sciences*: Vol. 21: Iss. 2, Article 16.

Available at: <https://jds.ads.org.tw/journal/vol21/iss2/16>

This Original Article is brought to you for free and open access by Journal of Dental Sciences. It has been accepted for inclusion in Journal of Dental Sciences by an authorized editor of Journal of Dental Sciences. For more information, please contact cpchiang@ntu.edu.tw.



Available online at <https://jds.ads.org.tw/journal/>

Digital Commons

journal homepage: <https://jds.ads.org.tw/journal/>



Original Article

Effect of zirconia nanopowders as functional fillers in dental adhesives on bonding durability and wear resistance to zirconia substrates

Ting-Hsun Lan ^{a,b*}, Chin-Yun Pan ^{b,c}, Yu-Feng Chen ^{b,d},
Chia-I Tiffany Yin ^b

^a Division of Prosthodontics, Department of Dentistry, Kaohsiung Medical University Hospital, Kaohsiung, Taiwan

^b School of Dentistry, College of Dental Medicine, Kaohsiung Medical University, Kaohsiung, Taiwan

^c Division of Orthodontics, Department of Dentistry, Kaohsiung Medical University Hospital, Kaohsiung Medical University, Kaohsiung, Taiwan

^d Division of Oral and Maxillofacial Surgery, Department of Dentistry, Kaohsiung Medical University Hospital, Kaohsiung, Taiwan

Received 5 August 2025; Final revision received 11 October 2025

Available online 1 April 2026

KEYWORDS

Zirconia nanopowder;
Dental adhesive;
Bond durability;
Wear resistance;
Shear bond strength

Abstract *Background/purpose:* A major cause of long-term failure in zirconia-based restorations is the degradation at the adhesive interface, often accelerated by hydrolytic and mechanical stress. This study investigated the effect of incorporating zirconia nanoparticles into a light-curable adhesive system to enhance interfacial durability and bonding performance to zirconia.

Materials and methods: Forty zirconia discs were treated with adhesive formulations containing zirconia nanoparticles at different weight ratios (0:10, 2:8, 5:5 and 8:2, labeled Pure, Z28A, 5Z5A and 8Z2A respectively). Following photopolymerization, solubility tests in deionized water and wear resistance assessments under cyclic abrasion were conducted up to 24 weeks and 48,000 cycles respectively. Shear bond strength (SBS) was also tested using 20 sintered zirconia specimens. Surface morphology, roughness and elemental composition were characterized via optical microscope, surface profilometry, scanning electron microscope.

Results: Immersion testing revealed that the weight loss of the Pure group slightly increased, whereas the Z28A group exhibited the least weight loss and superior stability during the long-term period after four weeks while further exhibiting minimal thickness change after the

* Corresponding author. School of Dentistry, College of Dental Medicine, Kaohsiung Medical University, 100 Shin-Chuan 1st Road, Sanmin District, Kaohsiung 807378, Taiwan.

E-mail address: tinghsun.lan@gmail.com (T.-H. Lan).

<https://doi.org/10.1016/j.jds.2025.10.011>

1991-7902/© 2026 Association for Dental Sciences of the Republic of China. Publishing services by Digital Commons. This is an open access article under the CC BY-NC-ND license (<http://creativecommons.org/licenses/by-nc-nd/4.0/>).

abrasion test. In SBS testing, although the Z28A group exhibited the highest mean bond strength, the difference was not statistically significant compared with that of the Pure group ($P > 0.05$). Z28A exhibited stable performance in abrasion, solubility, and bond strength, suggesting potential for oral applications in the future.

Conclusion: The enhanced performance of the zirconia nanopowder-containing adhesive, especially Z28A, demonstrated improved hydrolytic and mechanical stability at the zirconia crown–abutment interface, addressing a key challenge in long-term clinical success.

© 2026 Association for Dental Sciences of the Republic of China. Publishing services by Digital Commons. This is an open access article under the CC BY-NC-ND license (<http://creativecommons.org/licenses/by-nc-nd/4.0/>).

Introduction

A primary cause of the long-term failure of dental restorations, especially zirconia-based prostheses, is the degradation at the adhesive interface, and this is usually in the form of microleakage.^{1,2} This could be explained by a number of mechanisms: (1) poor bonding with interfacial gaps for bacterial and salivary penetration leading to secondary caries, marginal dissolution and hydrolytic degradation; (2) fatigue failure at the adhesive interface possibly leading to marginal debonding or chipping; (3) incompatibility between adhesive and zirconia materials' coefficients of thermal expansion with cyclic masticatory loading, leading to microcrack formation and consequent leakage; and (4) flawed adhesive procedures such as inadequate cleaning, drying or primer application, compromising interfacial integrity.^{3,4} A marginal gap (as shown in Fig. 1) of approximately 50~120 μm is generally considered clinically acceptable for dental crowns, although even minimal discrepancies have been associated with increased plaque accumulation, microleakage and a higher risk of secondary caries, underscoring the importance of minimizing the marginal gap wherever possible.⁵

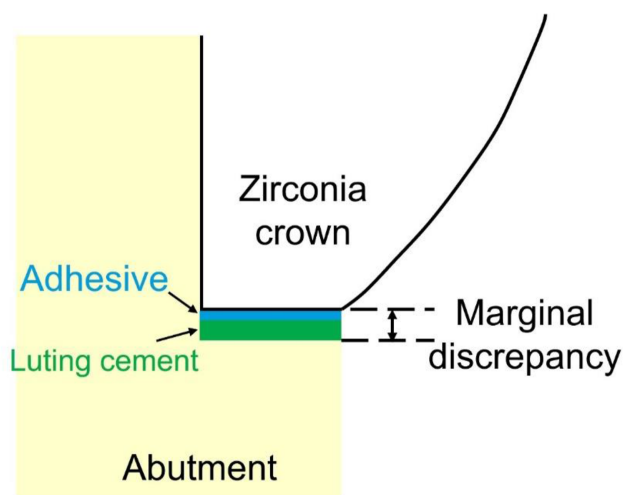


Figure 1 The schematic diagram of marginal discrepancy in dental restorations.

With the widespread use of digital workflows in dentistry, zirconia has emerged as a material of choice for fixed dental prostheses owing to its mechanical properties and esthetic potential; nevertheless, achieving a durable and hermetic seal at the zirconia–adhesive interface remains a significant clinical challenge. To improve mechanical and chemical bonds, various surface treatments have been employed in dental clinics or laboratories, such as airborne-particle abrasion (APA), tribochemical silica coating, low-fusion porcelain application, hot chemical etching, selective infiltration etching, laser irradiation, plasma spraying and glass ceramic spray deposition.⁶ Among these strategies, a combination of APA followed by 10-methacryloyloxydecyl dihydrogen phosphate (10-MDP) is widely regarded as the gold standard for zirconia bonding^{6,7} as this approach leverages the dual benefits of micro-mechanical retention from APA and chemical bonding via functional monomers. 10-MDP, a phosphate ester monomer, has emerged as the most effective coupling agent for bonding to yttria-stabilized tetragonal zirconia polycrystal ceramics^{8,9} as its molecular structure enables the formation of strong chemical bonds with zirconium oxide surfaces, facilitating durable adhesion between the zirconia substrate and resin-based materials.

This robust bond is essential for the adhesive's efficacy in maintaining restorations and preventing microleakage, so is expected to enhance the longevity and reliability of dental restorations; however, Takano et al.¹⁰ showed that micro-shear bond strength (μSBS) was significantly lowered after 10,000 thermocycles, particularly in the zirconia substrate with Scotchbond universal adhesive/RelyX universal dual-polymerizing resin cements. In that study, the μSBS decreased from 15.0 MPa to 3.0 MPa with only 35% of specimens surviving, demonstrating the need for continued research to improve the mechanical and chemical stability of zirconia primers and adhesive systems under long-term clinical conditions.

Solubility, abrasion and shear tests play an instrumental role in discerning materials and techniques that exhibit heightened resistance to failure, promoting the sustained functionality and longevity of dental restorations in clinical practice. Besides MDP, eighth-generation universal adhesives typically comprise various essential components, each contributing to their adhesive efficacy and resistance to external forces. Dimethacrylate resins¹¹ are one such example, providing mechanical strength and viscosity to

the adhesive layer while striking a harmonious balance between flexibility and rigidity, allowing the adhesive to accommodate dynamic oral forces in preserving structural integrity adeptly. These universal adhesives provide resistance to moisture and oral fluids thereby maintaining adhesive bond stability within a wet oral environment,^{12,13} as in the case of the hydrophilic monomer hydroxyethyl methacrylate (HEMA), which plays a crucial role in improving the adhesive's wettability, enabling it to spread evenly across the tooth surface and penetrate moist regions with its hydrophilic properties allowing the adhesive to adapt to the oral environment.¹⁴ While HEMA contributes positively to initial wetting and resin infiltration into moist dentin, it does not enhance and may even compromise the long-term hydrolytic stability of the adhesive interface.¹⁵ The Vitrebond™ Copolymer is another adhesive that substantially contributes to the overall durability of the adhesive bond, ensuring its ability to withstand the mechanical stresses and dynamic forces inherent in the oral environment^{13,16} while fillers can modify the adhesive's physical properties like viscosity and handling characteristics thereby contributing to its mechanical properties.¹³

In addition to the aforementioned chemical components, fillers are incorporated to improve the mechanical properties of adhesive systems and address the loss of bond strength caused by recurrent caries over time.¹⁷ Fillers can modify rheological and other properties such as reducing cost, enhancing strength, increasing viscosity, improving thermal and electrical conductivity, and enhancing heat and solvent resistance.¹⁸ They can also prevent excessive penetration into the matrix and reduce shrinkage during hardening. Traditionally, amorphous glass has been used as a filler, but in recent years, there has been a shift toward the use of various inorganic fillers.¹⁸ Of particular interest is the incorporation of functional fillers such as silica, hydroxyapatite nanorods, and TiO₂ and ZrO₂ nanoparticles into adhesive systems.^{17,19–23} Compared with other functional fillers such as silica or hydroxyapatite nanorods, zirconia nanoparticles have attracted increasing attention in dentistry owing to their excellent mechanical properties, biocompatibility and multifunctionality.¹⁷ Recently, their incorporation as fillers into dental adhesives has been proposed to enhance the mechanical performance of the resin matrix, reduce water sorption and solubility, and improve the bonding strength and long-term durability at the dentin–adhesive interface.^{17–19,22} Due to their high hardness and toughness, ZrO₂ nanoparticles can activate toughening mechanisms such as crack deflection and localized plastic deformation, thereby increasing both fracture and wear resistance. Additional benefits include their intrinsic radiopacity and potential antimicrobial effects when combined with other nanoparticles, which further add clinical value.^{17,20,24} Nevertheless, the particle size (typically 20–50 nm) might hinder infiltration into the collagen fibril network; high filler concentrations can lead to increased film thickness, phase separation, and reduced polymerization degree, while some studies report decreases in flexural or shear bond strength after aging or thermocycling.¹⁹ Overall, ZrO₂ nanoparticles demonstrate considerable promise as functional fillers in dental adhesives, but their optimal concentration, dispersion and surface treatment must be carefully controlled to ensure long-

term stability and reliable clinical performance.^{17–19,22} Lohbauer et al.¹⁹ showed that when nano-ZrO₂ was added to the composite system, it could improve the tensile strength, fracture toughness and resistance to hydrolytic degradation, while other studies have also reported that the addition of ZrO₂ could improve the shear bond strength.^{17,20,22,23} Although such effects of incorporating nanoparticles into adhesives on preventing microleakage have been rarely reported, extensive research is certainly warranted regarding the percentage of nanoparticles added to adhesive systems and their effects on anti-abrasion and anti-solubility.

This study aimed to explore innovative strategies for enhancing the wear-resistance and solubility stability of prosthetic margins, thereby reducing the risk of microleakage during long-term clinical use. To achieve this, dental adhesives incorporating various proportions of zirconia (ZrO₂) nanoparticles were formulated and evaluated through a series of mechanical and chemical tests, including abrasion resistance, solubility and shear bond strength assessments. It was hypothesized that the incorporation of zirconia nanoparticles would improve the mechanical properties and chemical stability of the adhesive layer, and that an optimal proportion of zirconia would yield the most balanced enhancement among these properties.

Materials and methods

Sample preparation

Commercial zirconia nanopowders (40 nm, TZ-3Y-E, Tosoh Corp, Tokyo, Japan) and a photo-polymerization adhesive bonding agent (Single Bond Universal Adhesive, 91125C, 3M ESPE, St. Paul, MN, USA) were precisely weighed, and a small amount of alcohol was added to the glass vial for premixing. The prepared mixture volume was standardized so that each batch was sufficient for fabricating ten specimens. The suspension was then sonicated in an ultrasonic cleaner (D9NL-801S, LEO Ultrasonic Co., New Taipei city, Taiwan) under 80 Watt and 4 kHz for 30 min. This process ensured thorough dispersion to create solutions for the four main test groups with ZrO₂ nanoparticles incorporated at different weight ratios to the adhesive: 0:10 (Pure), 2:8 (2Z8A), 5:5 (5Z5A), and 8:2 (8Z2A).

Round sintered zirconia disks (ϕ 12mm \times 4 mm in height) sourced from Vita (VITA Zahnfabrik, Säckingen, Germany) were meticulously polished stepwise by automatic polishing equipment (PM-200SA, Plusover, Kaohsiung, Taiwan) with water cooling at 180 rpm, using up to 600-grit SiC abrasive paper. Before applying the as-prepared solution to the specimen, an electronic balance was used to precisely measure the amount of solution absorbed by the brush. After applying the solution to the specimen, the same electronic balance was then used to measure the amount of solution remaining on the brush, thereby determining the exact amount of solution applied to the disc. Then, the 500 mg as-prepared solution was uniformly applied onto the disks with a micro brush, following a clockwise pattern; subsequently, it underwent light-curing (Elipar™ DeepCure-L, 3M ESPE, Seefeld, Germany) for 40 s at a distance of

1 cm, under a measured light intensity of approximately 1470 mW/cm² (430–480 nm), ensuring consistent polymerization conditions across all specimens. The curing light intensity (≈ 1470 mW/cm²) was confirmed according to the manufacturer's technical specifications (3M Technical Product Profile, 2020), ensuring standardized polymerization energy delivery and reproducibility among all test groups.

Abrasion test

Three comparative ratio solutions as previously mentioned were meticulously applied to 40 zirconia specimens (N = 10); subsequently, initial surface roughness was measured using a surface roughness measurement machine (SJ-310, Mitutoyo Corp., Kanagawa, Japan) to establish the baseline with the specimens being submerged in 50 mL of de-ionized water within a petri dish for the abrasion test. To emulate the effects of three years of brushing,²⁵ an abrasion test was conducted utilizing an abrasion tester (PAT-2012, PROES Co., Taichung, Taiwan) programmed for 48,000 cycles at a rate of 60 cycles per minute with a loading of 2 N. Following this rigorous testing regimen, the specimens were air-dried for 24 h at room temperature, and their post-test roughness measurement was meticulously reevaluated.

Solubility test

Each test group, consisting of 36 zirconia specimens alongside their respective ratio solutions, was subdivided into five submersion periods: 1, 2, 4, 12 and 24 weeks. Following the meticulous pre-pilot standardization procedure, the solution was meticulously applied to the zirconia disk and subjected to a light-curing process. Initial assessments encompassed precise measurements of each specimen's weight and comprehensive microscopic image evaluations; then, the specimens were placed within a petri dish containing deionized water, corresponding to the specified submersion duration. Upon completion of the required submersion time, the specimens were carefully removed and the 24-h air-drying procedure was conducted under a controlled laboratory atmosphere maintained at 23 ± 2 °C and $50 \pm 5\%$ relative humidity, then the specimens were reweighed to assess changes in mass with microscopic images being once again captured to facilitate a microscopic-level comparison of alterations induced by the applied solution.

Shear bond test

Twenty sintered square zirconia disks (VITA Zahnfabrik), each measuring $10 \times 10 \times 4$ mm³, were prepared and underwent a systematic polishing process that utilized 600-grit SiC paper. For the subsequent procedure, a uniform layer of the solutions was applied to one side of each zirconia disk using a micro brush; subsequently, two zirconia disks were carefully aligned, with the bonding agent sandwiched. A specialized mold was designed and customized to securely hold the zirconia specimens during the shear bond test with the crosshead speed set to align with the

vertically centered specimen and positioned as close as possible to the bonding interface. Three groups of specimens were prepared for comparison: an initial group (as-received), one subjected-to-abrasion testing, and one immersed in deionized water for four weeks. These were then subjected to the test using a universal testing machine (LR30KPlus, Lloyd Instruments Ltd., West Sussex, UK) at room temperature by operating with compressive loading at a crosshead speed of 1.0 mm/min. The force was applied to the bonding interface until it fractured, and the failure load was measured in Newtons that were then divided by the surface area (mm²) to calculate the shear bond strength in MPa.

Sample characterization

At every juncture in the experimental procedure, a digital optical microscope (OM, BX51, Olympus Corp., Tokyo, Japan) inspected the specimens' surface morphology and thickness of coating layers to assess the disparities between the pre-test and post-test conditions. By carefully monitoring the weight of the applied solution, the adhesive layer thickness of all specimens was maintained constantly while being measured on all four sides of each specimen, with five evenly distributed measurement points per side, and the mean value was calculated to obtain a representative average thickness. Furthermore, to delve deeper into the intricate nuances of the bonding structure within the solution, the morphology and the chemical compositions of the samples were examined by a scanning electron microscope (FE-SEM, JSM-7001F, JEOL Ltd., Tokyo, Japan) and an attached energy dispersive spectroscopy (EDS).

Statistical analysis

The results between groups were statistically analyzed via one-way analysis of variance (ANOVA) with a significance level of $P < 0.05$, followed by *post hoc* comparisons using the Tukey test. Paired *t*-test was used to analyze the surface roughness and thickness before and after the abrasion test. These analyses were performed using IBM SPSS Statistics for Windows, Version 20 (IBM Corp., Armonk, NY, USA) and the required sample size was calculated using G*Power 3.1.9.7 with an assumed effect size of 0.5, alpha of 0.1 and power of 0.8, indicating that N = 10 per group was required.

Results

Table 1 lists the surface roughness (Ra) and thickness of pre- and post-abrasion testing, and in the case of the Pure ratio test group, the pre-test Ra registered at 0.40 ± 0.20 μm, a figure that escalated to 0.45 ± 0.22 μm post-test. The thickness of the Pure group decreased from 19.46 ± 5.85 μm before testing to 14.40 ± 4.52 μm after abrasion. For the sample 2Z8A, the surface roughness was recorded at 0.99 ± 0.35 μm prior to abrasion testing and slightly escalated to 0.82 ± 0.30 μm afterward, resulting in a 10.51 % decrease. Sample 2Z8A exhibited a decrease in thickness from 21.26 ± 6.13 μm prior to testing to 19.53 ± 5.79 μm after abrasion. The sample 5Z5A exhibited

Table 1 The surface roughness (Ra) and thickness before and after abrasion test.

Group	Roughness (μm)		Thickness (μm)		Strokes
	Before	After	Before	After	
Pure (N = 10)	$0.40 \pm 0.20^{\text{Ca}}$	$0.45 \pm 0.22^{\text{Ea}}$	$19.46 \pm 5.85^{\text{Fe}}$	$14.40 \pm 4.52^{\text{Ge}}$	48,000
2Z8A (N = 10)	$0.99 \pm 0.35^{\text{Bb}}$	$0.82 \pm 0.30^{\text{Dc}}$	$21.26 \pm 6.13^{\text{Ff}}$	$19.53 \pm 5.79^{\text{Gf}}$	48,000
5Z5A (N = 10)	$1.02 \pm 0.57^{\text{ABd}}$	$1.11 \pm 0.70^{\text{Dd}}$	$18.62 \pm 4.92^{\text{Fg}}$	$14.98 \pm 4.97^{\text{Gg}}$	48,000
8Z2A (N = 10)	$1.53 \pm 0.68^{\text{A}}$	—	$17.36 \pm 6.43^{\text{F}}$	—	<100

*One-way ANOVA and paired *t*-test (before/after); Different uppercase letters in the same column and lowercase letters in the same row indicate statistical significance between groups ($P < 0.05$; *post hoc* Tukey test). No statistical comparisons were made between cells in different rows and columns.

a pre-test surface roughness measurement of $1.02 \pm 0.57 \mu\text{m}$, which subsequently rose to $1.11 \pm 0.70 \mu\text{m}$ post-test, signifying an 11.75% increment. After abrasion, the thickness of sample 5Z5A was reduced from its initial value of $18.62 \pm 4.92 \mu\text{m}$ to $14.98 \pm 4.97 \mu\text{m}$. The surface roughness and thickness of sample 8Z2A pre-test was $1.53 \pm 0.68 \mu\text{m}$, $17.36 \pm 6.43 \mu\text{m}$; however, after less than 100 abrasions, the coatings on all the specimens had peeled off, revealing that this ratio could not achieve the desired anti-abrasion effect.

Fig. 2 shows the cross-sectional view of the thickness of four different ratio samples observed under an optical microscope with the thickness of all samples being approximately $20 \mu\text{m}$. The 2Z8A group thickness was slightly higher than that of the pure group; however, as the amount of

zirconia nanopowder increased, the thickness tended to decrease. Further microscopic examination as shown in Fig. 3 revealed noteworthy alterations in the before-and-after images of all test groups following the abrasion test. OM images indicated that all test groups exhibited discernible scratch marks following the rigorous abrasion test, collectively contributing to an overall increase in surface roughness values. Specifically, the post-test microscopic image of the pure solution revealed an increased presence of exposed bonding agent particles, resulting in a discernibly uneven or bumpy surface texture compared to its pre-test counterpart. In the initial microscopic analysis of the 2Z8A solution, small ZrO_2 particles were discernible; however, a marked increase in the abundance of ZrO_2 particles became evident in the

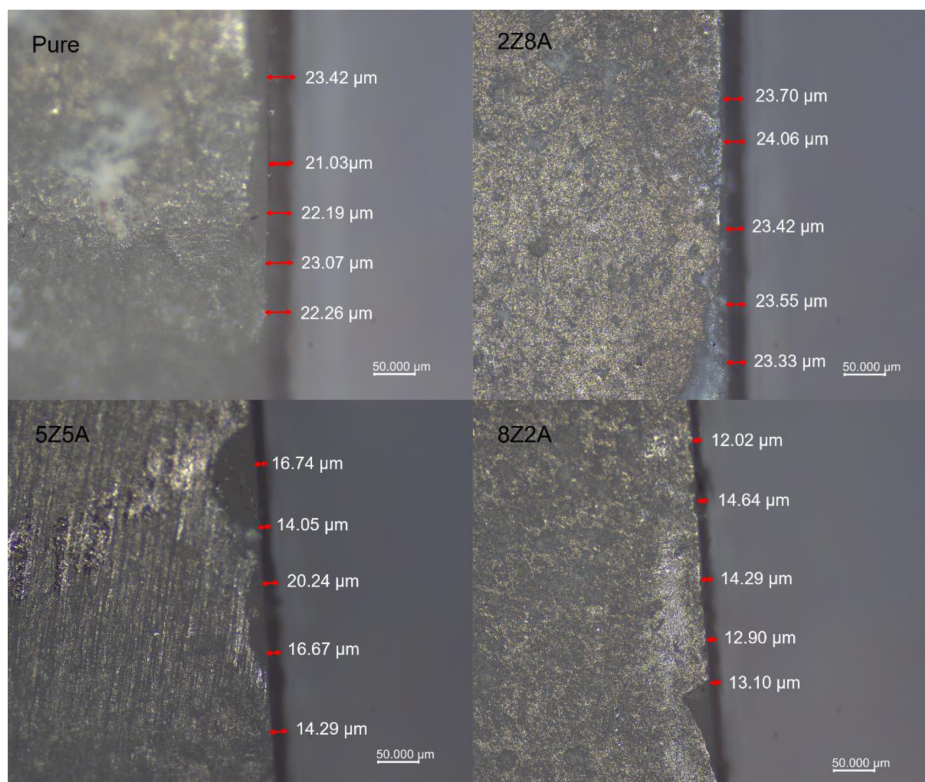


Figure 2 Observation of coating layer thickness with different proportions of zirconia nanoparticles using an optical microscope.

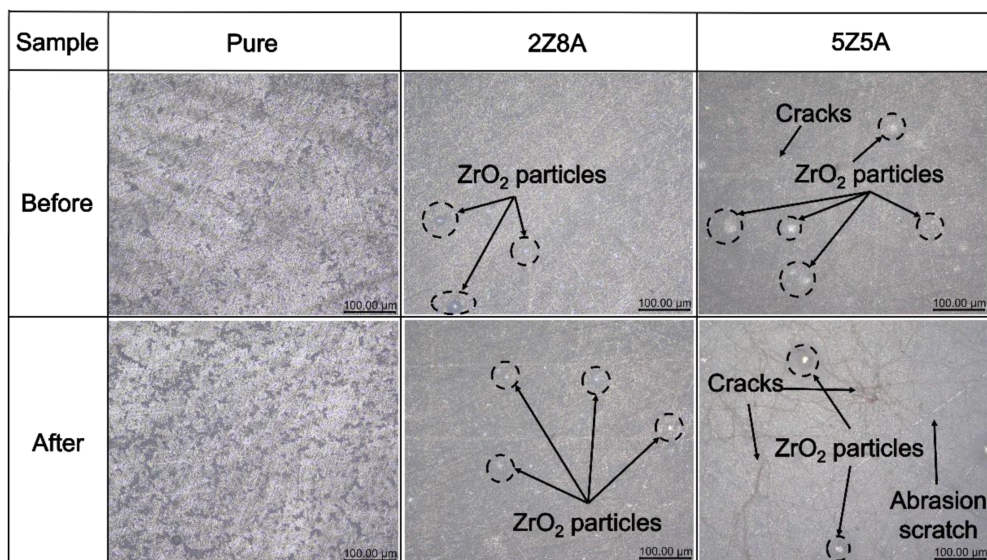


Figure 3 Comparison of zirconia specimens with bonding agent solution before and after abrasion test.

microscopic images subsequent to the abrasion test. When examining the 5Z5A solution under a microscope, a significant observation came to light: there was a conspicuous increase in the size and visibility of ZrO_2 particles.

This occurrence could be traced back to the relatively higher concentration of zirconia powders compared to the bonding agents within the ratio. Furthermore, the microscopic examination revealed the presence of distinctly crazed lines; intricate patterns known to be associated with dry cracking and serving as indicators of possible structural vulnerabilities within the material where such irregularities are often attributed to an imbalance in the powder-to-liquid ratio, a condition that can arise as a consequence of the light-curing phase.

Fig. 4 depicts the average weight loss for each group concerning the duration of submersion. The Pure test group in the first week demonstrated the least weight loss, but

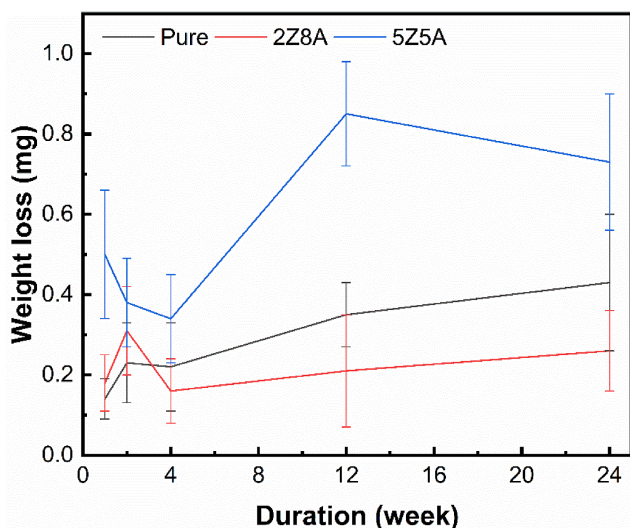


Figure 4 Correspondent weight loss of pure, 2Z8A and 5Z5A specimens after being soaked for different durations.

over time, it displayed a subtly increasing trend, while in contrast, the 2Z8A group exhibited an initial mass change that was slightly higher than that of the Pure group. During the two-week submersion period, the 2Z8A group exhibited a gradual increase in weight loss, although after the fourth week, the weight loss decreased, and with prolonged immersion, it showed a slight upward trend again. During the initial immersion period, all groups exhibited weight loss, primarily attributable to the leaching of unpolymerized monomers, fillers, and other extractable constituents from the adhesive matrix. The 5Z5A group presented a markedly greater early weight loss, which is likely associated with its high zirconia nanoparticle content. Such elevated filler loading may have induced microstructural irregularities—including crazing or microcracks—during the light-curing process, thereby facilitating increased water ingress and accelerated leaching. This mechanism could explain the substantial weight reduction observed up to the 4-week time point. After four weeks, both Pure and 2Z8A groups showed a more gradual and stable weight loss trend; however, the 5Z5A group remained unstable, which might be due to the excessive content of nanoparticles, affecting the dynamic equilibrium of sorption and solubility behavior. Notably, the 2Z8A group consistently showed the lowest average weight loss at 24 weeks, which could be attributed to its proper zirconia concentration, resulting in reinforcement of the polymer matrix and enhanced hydrolytic resistance. Conversely, the 5Z5A group exhibited a more dramatic pattern, with an initial slight decrease in weight mass up until the four-week mark, at which point the weight loss escalated substantially; then, the trend stabilized and eventually exhibited a decline in weight loss after the 12-week mark. In summary, these observations underscore the distinctive patterns of mass change exhibited by each test group during the course of the submersion test, shedding light on their respective responses to prolonged exposure to water.

The SEM images (Fig. 5) captured at various time intervals reveal a fascinating narrative of the evolving

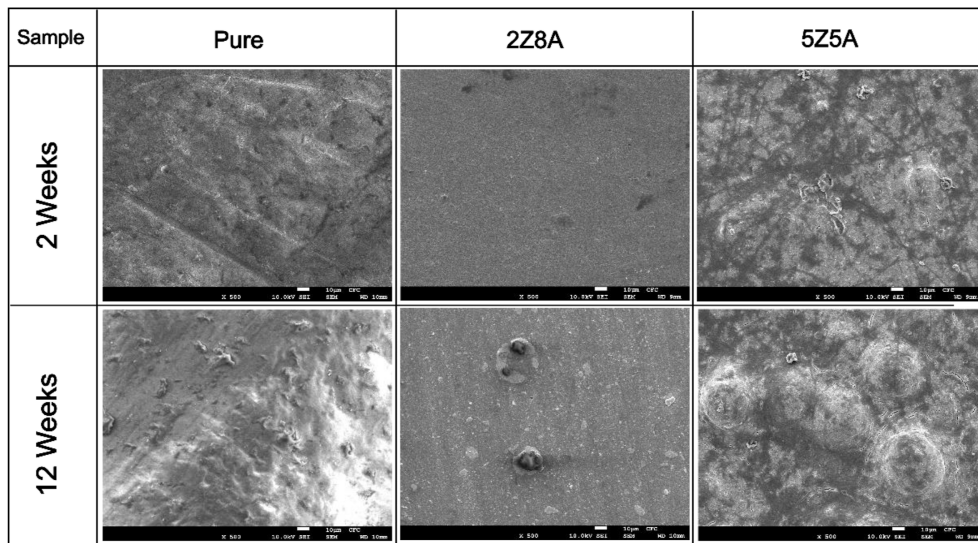


Figure 5 Scanning electron microscope (SEM) images of specimens with zirconia nanoparticles to bonding agent solution after the solubility test for 2 weeks and 12 weeks at 500x magnification.

interactions among the solution’s components in the presence of water over different durations. In the case of the Pure bonding agent, the visual record documents a relatively minimal degree of change consistent with the anticipated gradual bonding dissolution that unfolds over time; conversely, the 2Z8A solution exhibited a gradual and discernible progression in the dissolution process with this evolution being marked by the increasing prominence and visibility of zirconia particles as time elapsed. Remarkably, the 5Z5A solution presented the most pronounced transformation where the zirconia particles exhibited a propensity to aggregate, forming distinct clusters within their surrounding particles. This striking alteration in particle distribution underscored the dynamic nature of the interactions occurring within this solution.

The SBS of the three groups is listed in Table 2; the 2Z8A test group yielded a markedly higher shear bond strength of 5.49 MPa. This outcome decisively illustrates that this particular solution formulation resulted in a substantially

more robust bond compared to using the Pure bonding agent alone. The elevated SBS stands as tangible evidence of an advanced level of adhesion between the zirconia specimens, indicative of heightened bonding efficacy. Finally, a distinct trend emerged within the 5Z5A test group, where equal distribution of zirconia nanopowders and bonding agent (5:5) comprised the adhesive solution. The SBS, in this case, exhibited a noteworthy reduction, measuring at 2.38 MPa in stark contrast to the other two groups. ANOVA revealed a statistically significant factor influencing fracture load ($P < 0.05$), and upon closer examination, when comparing the Pure group to 2Z8A, the difference did not reach statistical significance, while in contrast, the comparison between 5Z5A and the other two test groups yielded statistically significant disparities. Additionally, two groups of specimens were tested in the SBS test: one group was subjected to an abrasion test, and the other group was subjected to a four-week immersion test. These SBS results also showed that the 2Z8A group had the highest value, while further revealing that the SBS of the Pure group weakened over time in the presence of water, with statistical significance ($P < 0.05$). The 2Z8A group maintained its superiority over the other groups in both the abrasion test and after four-week immersion, but the results were not statistically different from the initial data ($P > 0.05$).

Fig. 6 shows the EDS line scan analysis results of sample 2Z8A at different locations. It can be seen from the composition analysis of the bonding agent in the figure on the left that there is not much difference in the distribution of elements such as carbon, oxygen, silicon, phosphorus and zirconium; however, in the figure on the right, phosphorus and zirconium are significantly increased in the central range of ZrO_2 nanoparticles. It can be speculated that the 10-MDP in the bonding agent does indeed bond phosphorus and zirconium together, ensuring material homogeneity, which is crucial for quality control in dental prosthetic repair applications.

Table 2 Shear bond strength values of three groups.

Group	Shear bond strength* (MPa) Initial	Shear bond strength* (MPa) After abrasion test	Shear bond strength* (MPa) After immerse 4 weeks
Pure	4.89 ± 0.76 ^{Aa}	3.83 ± 0.96 ^{ABb}	3.19 ± 0.95 ^{Bb}
2Z8A	5.49 ± 1.64 ^{Āa}	5.82 ± 0.76 ^{Āa}	6.58 ± 0.93 ^{Āa}
5Z5A	2.38 ± 0.64 ^{Āb}	2.53 ± 0.56 ^{Āc}	2.99 ± 0.42 ^{Āb}

*One-way ANOVA (three independent groups); Different lower-case letters in the same column and uppercase letters in the same row indicate statistical significance between groups ($P < 0.05$; *post hoc* Tukey test). No statistical comparisons were made between cells in different rows and columns.

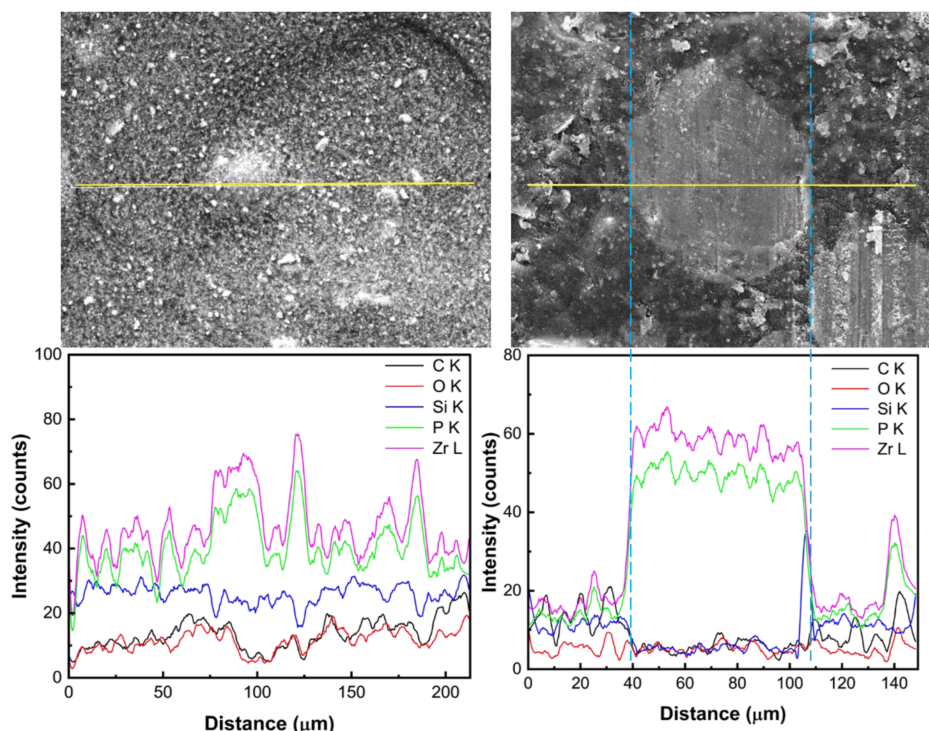


Figure 6 Energy dispersive spectroscopy (EDS) analysis of specimens with zirconia nanoparticles to bonding agent solution. (Left: solution matrix; Right: zirconia nanoparticles mixed with bonding agent).

Discussion

In essence, the abrasion test evaluated the ability of the dental materials to withstand the regular wear-and-tear encountered in the oral cavity while ensuring their longevity, with the shear bond test measuring the force required to break the bond between the dental restoration material and the tooth structure. Among the four samples, Z28A exhibited the minimal changes in surface roughness and thickness before and after the abrasion test. Moreover, an increase in the proportion of ZrO₂ nanopowder was associated with a decline in wear resistance. Compared to the other groups, Z28A also showed the most stable trend in weight loss from week 4 to week 24, indicating its potential for long-term use, and although the initial Z28A group exhibited the numerically highest mean bond strength, it was not statistically significant compared with the Pure group ($P > 0.05$) but still maintained its advantage and outperformed the other groups after abrasion and immersion tests. Taken together, these findings suggest that incorporating 20 wt.% zirconia nanopowder into the adhesive is an appropriate and effective ratio in a series of laboratory tests.

Scotchbond Universal adhesive comprises various essential components, each playing a pivotal role in its adhesive prowess. With proper ratio mixture, new products (Z28A) can modify the adhesive's physical properties like viscosity and handling characteristics while also contributing to its mechanical properties. Notably, Nagaoka et al.²⁶ conducted a study where the incorporation of pure zirconia nanoparticles into commercially available products already fortified with a substantial amount of silica fillers showed promise. The foundation of this research hinged on

the potential establishment of a direct bond between zirconia and phosphoric or carboxylic adhesive monomers, where the lack of zirconia nanoparticles made it dissolve easily in solubility tests and caused it to lose wear resistance and load-carrying capacity normally provided by this nanopowder in wear tests.

Although some reports indicate that non-MDP-containing self-adhesive resin cement showed increased bonding strength when used with MDP-containing primer on zirconia ceramics,²⁷ it is widely believed that the addition of 10-MDP enhances bond strength with zirconia. To date, the detailed composition of Scotchbond Universal Adhesive provided by the manufacturer remains unclear owing to undisclosed Intellectual Property Rights; still, it is known that the phosphate group of 10-MDP can bond with zirconia. In contrast, the double carbon bond at the other end mainly participates in copolymerization with the resin matrix in dental restorative materials. As shown in Fig. 7, in the Pure group, 10-MDP molecules could form bonds with the underlying zirconia substrate. When an appropriate proportion of zirconia particles is mixed with the primer solution, although a few bonds with the underlying zirconia substrate may be sacrificed, lateral capture of the zirconia particles forms a more stable scaffold, which could result from the phosphate groups in 10-MDP forming ionic bonds with zirconia in addition to hydrogen bonding interactions between the P=O of the 10-MDP monomers and zirconia, further contributing to improved hydrolysis and abrasion resistance as suggested by prior reports,²⁶ although in the 5Z5A group, the excessive amount of zirconia particles occupying the binding sites for the phosphate group and the zirconia base tends to reduce the coating layer's stability.

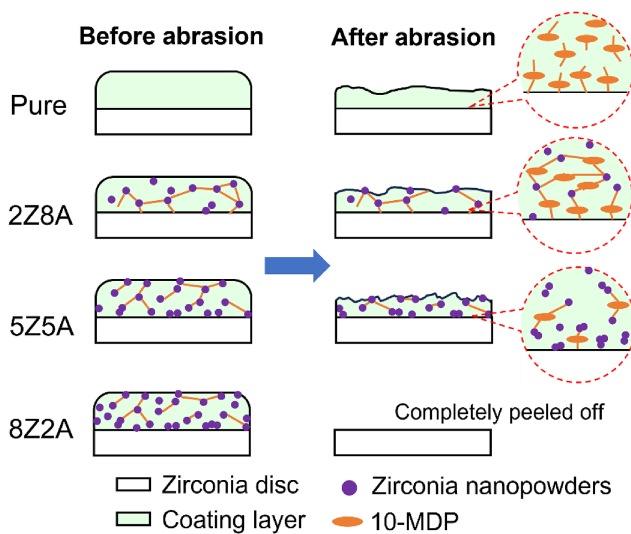


Figure 7 Schematic illustrating the interactions after abrasion of coating layers with different proportions on a zirconia substrate.

A similar reinforcing effect was observed in previous research by Lohbauer et al., who found that incorporating 20 wt.% zirconia nanoparticles as nanofillers was more effective in enhancing bond strength when mixed into the primer solution.¹⁹ During the polymerization of dental resin-based materials, molecular density increases as polymer chains form, ultimately resulting in a reduction in material volume. The internal stresses and even microcracks that develop during this shrinkage impact bond strength and durability,²⁸ but incorporating a small amount of zirconia nanoparticles dispersed with the adhesive could not only enhance the surface energy of the adhesive layer but act as a barrier to microcrack propagation as the microcracks extend as well, explaining why 20 wt.% (2Z8A) showed the least weight loss and achieved higher bond strength after four weeks of immersion. When the zirconia content exceeded 20% however, it disrupted the delicate balance of properties within the mixture, leading to multiple adverse effects.

The incorporation of zirconia nanopowders in the 2Z8A solution fortified its resistance to abrasion and load with the particles acting as a protective shield, mitigating the impact of abrasive forces during the abrasion test. In contrast, both the Pure bonding agent and the 5Z5A solution lacked this protective effect, with the latter facing possible issues due to oversaturation, while the 2Z8A mixture attained a superior equilibrium between the bonding agent's properties and zirconia nanopowder, ensuring a more uniform and consistent balanced performance during the tests. In contrast, the Pure bonding agent lacked the reinforcing attributes of zirconia nanoparticles, while the 5Z5A solution could exhibit non-uniform consistency due to excessive nanopowder content. Moreover, the 2Z8A ratio optimized the bonding properties between the bonding agent and the dental surface, yielding a stronger and more resilient bond; conversely, both the Pure bonding agent, devoid of zirconia nanoparticles as well as the 5Z5A

solution that was oversaturated with them produced less effective bonds.

Clinically, marginal gaps between 50 and 120 μm are generally accepted, but smaller discrepancies are desirable to prevent cement dissolution and bacterial penetration. The adhesive layer containing zirconia nanoparticles ($\approx 20 \mu\text{m}$) is therefore unlikely to increase marginal elevation or interfere with restoration seating. In particular, the 2Z8A formulation exhibited superior mechanical stability and hydrolytic resistance, demonstrating minimal surface roughness change and thickness loss after long-term abrasion and immersion. The homogeneous dispersion of zirconia nanoparticles acted as nano-reinforcing fillers, enhancing load distribution and micro-crack deflection within the polymer matrix. Simultaneously, the chemical interactions formed a denser, less permeable interface that limited water uptake and leaching of unreacted monomers. These combined effects are expected to facilitate better marginal adaptation and long-term adhesion by maintaining structural integrity, minimizing microleakage, and reducing plaque accumulation at the tooth–prosthesis interface. The minimal reduction in thickness also indicated sufficient wear resistance, further contributing to the prevention of decay. If a layer of 2Z8A were applied between the prosthesis and the abutment tooth and maintained through daily tooth brushing, it could potentially reduce the risk of microleakage during long-term use, although further *in vivo* studies are necessary to confirm this effect.

Although the SBS of 5Z5A did not change significantly between initial and post-test values, its strength remained consistently and markedly lower than those of Pure and 2Z8A. This is presumably because the excessive nanoparticles prevent the adhesive from distributing uniformly, thereby compromising its ability to establish strong bonding with the substrate surface. Beketova et al.²⁹ also showed that excessive particle content could block light penetration and affect the degree of polymerization. In aqueous environments, crack propagation may be forced to bypass the particle clusters, inadvertently generating additional cracks (as shown in Fig. 3). This not only reduces shear bond strength but also causes water entrapment within the cracks, making complete evaporation difficult thereby resulting in increased weight after immersion. Ultimately, these effects lead to greater weight loss, reduced shear bond strength, and increased surface roughness. Especially during the solubility test, the non-linear (“zig-zag”) pattern observed, especially in the 5Z5A group, likely resulted from the interplay between two concurrent processes: (1) water sorption and swelling of the adhesive matrix, which temporarily increases mass, and (2) leaching of unreacted monomers and hydrolytic degradation products, which reduces specimen weight. The balance between these opposing mechanisms could create apparent fluctuations rather than a smooth degradation curve. Additionally, the drying procedure (24 h at room temperature) might have contributed to variability, as incomplete evaporation of absorbed water in highly porous specimens could transiently mask true weight loss. The test group 5Z5A, characterized by an oversaturation of zirconia nanoparticles, displayed higher initial roughness than groups Pure and 2Z8A, serving as a vital foundation for our analysis, and further supported by the insights presented in Lee et al.’s

study³⁰ which emphasized the pivotal role of zirconia surface roughness; the surface texture significantly augments the contact area with moisture, although an excessive amount of zirconia nanoparticles could engender heightened interactions between these particles, manifesting as abrasive effects when the particles rub against each other or the dental surface during the abrasion test, further contributing to the increase in surface roughness.

At the 8:2 ratio (8Z2A), the excessive zirconia nanoparticle content appears to have produced several detrimental effects on the adhesive system. Firstly, the high filler loading likely promoted poor dispersion and agglomeration during mixing and light curing thereby creating microvoids and localized stress concentrations that compromised coating integrity and accelerated delamination under abrasive conditions. Secondly, the disproportionate filler content reduced the continuity of the resin matrix, and with insufficient adhesive resin to encapsulate and stabilize the nanoparticles, the polymer network became discontinuous, thereby weakening its mechanical properties and diminishing its resistance to hydrolytic degradation. Thirdly, an overload of zirconia nanoparticles could have physically occupied or shielded critical surface sites, impeding effective 10-MDP bonding with the zirconia substrate and thus reducing the chemical anchorage essential for long-term adhesion; these results are consistent with the findings of Sangh et al.¹⁸ Collectively, these factors explain the inferior performance of the 8Z2A group compared with both Pure and lower-filler groups, underscoring the presence of an improper filler concentration. Moderate incorporation (2Z8A) enhanced abrasion resistance and hydrolytic stability, whereas excessive particle loading (5Z5A even 8Z2A) disrupted the balance of the system, leading ultimately to compromised mechanical performance. As a consequence, the results of this study only partially support the initial hypothesis that incorporating zirconia fillers would enhance overall adhesive performance, and while the addition of zirconia nanoparticles did not consistently improve all mechanical and chemical properties, an optimal formulation (2Z8A) was identified, demonstrating a balanced enhancement in both mechanical reinforcement and chemical stability. These findings reveal the benefits of nanoparticle incorporation depend strongly on precise compositional control to achieve synergistic effects without compromising other critical adhesive characteristics.

The limitation of this study was the simulation of the oral environment to control the mixture of each specimen, so future work should establish a control group consisting of composite resin and various bonding agent brands for comparison as well as different surface treatments of zirconia. Furthermore, thermal cycling is a critical aging factor in the clinical setting, and its absence might have limited extrapolation of the findings to real-world applications. Future studies should therefore incorporate thermal cycling protocols—ideally in combination with long-term water storage and pH cycling—to better simulate the intraoral environment and validate the durability of the 2Z8A formulation under simulated clinical aging conditions. This innovative mixing method demonstrates potential for use not only in prosthetic restorations but for future

applications as a coating on the inner layer of zirconia crowns to enhance retention as well.

Adding an appropriate proportion of ZrO₂ nanoparticles to the adhesive has a positive effect. The 2Z8A solution test group, with its superior reinforcement, enhanced cohesion, improved abrasion resistance, uniformity and optimized bonding properties while outperforming the other groups in both solubility and abrasion tests. These collective advantages account for their more favorable results over both pure bonding agent and 5Z5A solution test groups.

Declaration of competing interest

The authors have no conflicts of interest relevant to this article.

Acknowledgments

This research is grateful for the support of the National Science and Technology Council by fund MOST110-2813-C-037-025-B and Kaohsiung Medical University Hospital by KMH110-0R75, KMH113-3R63 and KMH-DK(B)114006–1. The authors also appreciate the assistance from Core Facility Center (National Cheng Kung University, Taiwan) in operating the SEM/EDS instrument.

References

1. Kaczor K, Gerula-Szymańska A, Smektała T, Safranow K, Lewusz K, Nowicka A. Effects of different etching modes on the nanoleakage of universal adhesives: a systematic review and meta-analysis. *J Esthetic Restor Dent* 2018;30:287–98.
2. Deng D, Yang H, Guo J, Chen X, Zhang W, Huang C. Effects of different artificial ageing methods on the degradation of adhesive-dentine interfaces. *J Dent* 2014;42:1577–85.
3. Mokeem LS, Garcia IM, Melo MA. Degradation and failure phenomena at the dentin bonding interface. *Biomedicines* 2023; 11:1256.
4. Liu Y, Xu Y, Su B, Arola D, Zhang D. The effect of adhesive failure and defects on the stress distribution in all-ceramic crowns. *J Dent* 2018;75:74–83.
5. Kim TG, Kim S, Choi H, Lee JH, Kim JH, Moon HS. Clinical acceptability of the internal gap of CAD/CAM PD-AG crowns using intraoral digital impressions. *BioMed Res Int* 2016;2016: 7065454.
6. Peng TY, Kang CM, Feng SW, Hung CY, Iwaguro S, Lin DJ. Effects of glass-ceramic spray deposition manipulation on the surface characteristics of zirconia dental restorations. *Ceram Int* 2022; 48:29873–81.
7. Janson M, Bassier V, Liebermann A, Schoppmeier CM, Gregorio-Schininà MD. Composite repair on zirconia: influence of different sandblasting pretreatments and various universal adhesives on shear bond strength. *J Adhesive Dent* 2025;27: 53–64.
8. Scaminaci Russo D, Cinelli F, Sarti C, Giachetti L. Adhesion to zirconia: a systematic review of current conditioning methods and bonding materials. *Dent J* 2019;7:74.
9. Klaisiri A, Maneenacarith A, Jirathawornkul N, Suthamprajak P, Sriamporn T, Thamrongananskul N. The effect of multiple applications of phosphate-containing primer on shear bond strength between zirconia and resin composite. *Polymers* 2022;14:4174.

10. Takano S, Takahashi R, Tabata T, Zeng C, Ikeda M, Shimada Y. Bonding performance of universal adhesive systems with dual-polymerising resin cements to various dental substrates: in vitro study. *BMC Oral Health* 2025;25:101.
11. 3M Oral Care. 3M™Scotchbond™universal Plus Adhesive technical product profile. *Tech Product Profile*. 2020 https://www.3m.com/3M/en_US/dental-us/featured-products/scotchbond-universal-plus/.
12. Bahrololumi N, Beglou A, Najafi-Abbrandabadi A, Sadr A, Sheikh-Al-Eslamian SM, Ghasemi A. Effect of water storage on ultimate tensile strength and mass changes of universal adhesives. *J Clin Exp Dent* 2017;9:e78–83.
13. Scotchbond™ Universal adhesive: technical product profile. <https://multimedia.3m.com/mws/media/7547510/scotchbond-universal-adhesive-technical-product-profile.pdf>; 2013.
14. Alex G. Universal adhesives: the next evolution in adhesive dentistry? *Comp Cont Educ Dent* 2015;36:15–40.
15. Staxrud F, Valen H. Potential of «universal» bonding agents for composite repair. *Biomater Investig Dent* 2022;9:41–6.
16. Costa DM, Somacal DC, Borges GA, Spohr AM. Bond capability of universal adhesive systems to dentin in self-etch mode after short-term storage and cyclic loading. *Open Dent J* 2017;11:276–83.
17. Aljamhan AS, Alrefeai MH, Alhabdan A, et al. Interaction of zirconium oxide nanoparticle infiltrated resin adhesive with dentin conditioned by phosphoric acid and Er, Cr: YSGG laser. *J Appl Biomater Funct Mater* 2022;20:22808000221087349.
18. Sanghvi MR, Tambare OH, More AP. Performance of various fillers in adhesives applications: a review. *Polym Bull* 2022;79:10491–553.
19. Lohbauer U, Wagner A, Belli R, et al. Zirconia nanoparticles prepared by laser vaporization as fillers for dental adhesives. *Acta Biomater* 2010;6:4539–46.
20. Felemban NH, Ebrahim MI. The influence of adding modified zirconium oxide-titanium dioxide nano-particles on mechanical properties of orthodontic adhesive: an in vitro study. *BMC Oral Health* 2017;17:43.
21. Siwińska-Ciesielczyk K, Andrzejczak A, Jesionowski T, Gierz Ł, Marcinkowska A, Robakowska M. New insights into the application of biocompatible (un)modified TiO₂ and TiO₂-ZrO₂ oxide fillers in light-curing materials. *Materials* 2024;17:2908.
22. Al-Saleh S, Alateeq A, Alshaya AH, et al. Influence of TiO₂ and ZrO₂ nanoparticles on adhesive bond strength and viscosity of dentin polymer: a physical and chemical evaluation. *Polymers* 2021;13:3794.
23. Al-Saleh S, Vohra F, Alateeq A, et al. Strength of fiber posts with experimental TiO₂ and ZrO₂ particle bonding—an SEM, EDX, rheometric and push-out strength study. *Coatings* 2022;12:1176.
24. Khan AS, Alhamdan Y, Alibrahim H, et al. Analyses of experimental dental adhesives based on zirconia/silver phosphate nanoparticles. *Polymers* 2023;15:2614.
25. Garza LA, Thompson GA, Cho SH, Berzins DW. Effect of toothbrushing on shade and surface roughness of extrinsically stained pressable ceramics. *J Prosthet Dent* 2015;115:489–94.
26. Nagaoka N, Yoshihara K, Feitosa VP, et al. Chemical interaction mechanism of 10-mdp with zirconia. *Sci Rep* 2017;7:45563.
27. Go EJ, Shin Y, Park JW. Evaluation of the microshear bond strength of mdp-containing and non-mdp-containing self-adhesive resin cement on zirconia restoration. *Operat Dent* 2019;44:379–85.
28. Wang Z, Zhang X, Yao S, Zhao J, Zhou C, Wu J. Development of low-shrinkage dental adhesives via blending with spiroorthocarbonate expanding monomer and unsaturated epoxy resin monomer. *J Mech Behav Biomed Mater* 2022;133:105308.
29. Beketova A, Tzanakakis EGC, Vouvoudi E, et al. Zirconia nanoparticles as reinforcing agents for contemporary dental luting cements: physicochemical properties and shear bond strength to monolithic zirconia. *Int J Mol Sci* 2023;24:2067.
30. Lee JH, Kim SH, Han JS, Yeo IL, Yoon HI. Optical and surface properties of monolithic zirconia after simulated toothbrushing. *Materials* 2019;12:1158.